# Catalytic activity of poly(amino-organosiloxane)s

**Noboru Koyama, Yukihiko Ueno, Yasunori Sekiyama, Koji Ikeda and Yoshiro Sekine**

*Department of Chemistry, Waseda University, Ohkubo, Shinjuku-ku, Tokyo, Japan*

*(Received 22 December 1984)*

The poly(amino-organosiloxane)s (PAOS) form PAOS–Cu(II) complexes. The copper catalysed oxidation of ascorbate and hydroquinone by molecular oxygen was studied in the presence of PAOS. It was found that the addition of PAOS enhances the catalytic efficiency of Cu(II). The PAOS–Cu(II) catalysed reaction, unlike the Cu(II) catalysed reaction, becomes zero-order in the substrate concentration at relatively low concentration of substrate and exhibits Michaelis–Menten kinetics, which indicates the existence of a catalyst–substrate complex. This catalytic activity is similar to the poly(L-histidine)–Cu(II) catalysed reaction described by Pecht and Levitski. The specific effect of PAOS on the Cu(II) catalysed reactions is interpreted by the conformation of PAOS in aqueous solution, which is dependent on the flexibility and hydrophobicity of the PAOS main chain. In order to investigate the conformation of PAOS in aqueous solution, the decarboxylation of 6-nitrobenzisoxazole-3-carboxylate anion was studied, and it was found that the conformation of PAOS is easily controlled by altering the pH, the coordination to Cu(II) ions and the hydrophobicity of PAOS.

**(Keywords: siloxane; complex; catalyst; Michaelis–Menten; decarboxylation; conformation)**

## INTRODUCTION

The poly(organosiloxane)s (POS) are known to have a flexible main chain and their glass transition temperatures ($T_g$) are very low. For example, the $T_g$ of poly(dimethyl siloxane) (PDMS) is $-120$ to $-130$°C (ref. 1). PDMS has a hydrophobic main chain because of its Si–Me bonds. There have been some reports about water-soluble POS[2], but few reports related to POS having amino groups[3]. Poly(amino-organosiloxane) (PAOS) is water-soluble and besides has the ability to coordinate to metal ions. Compared with the carbon polymer, the PAOS main chain is more flexible and hydrophobic. When the catalytic efficiency of PAOS as a polymer–metal complex is studied, the formation of hydrophobic domains that are formed by PAOS affect its catalytic activity. Concerning carbon polymers, the hydrophobic domains that are formed by their side chains have been discussed[4]. It is simple synthesis for PAOS to introduce hydrophobic DMS into the PAOS main chain. The PAOS main chain is so flexible that the conformation of PAOS in aqueous solution is easily changed. For instance, when PAOS–Cu(II) complex is formed, the conformation of PAOS becomes compact. In the low pH region, the amino groups of PAOS become cationic groups by protonation, and then the conformation of PAOS becomes loose because of electrostatic repulsion. It was found that the specific effects of PAOS on copper catalysed oxidation could be attributed to the variation of PAOS conformation in aqueous solution. In order to study the factors concerned with the control of conformation of PAOS, the decarboxylation of carboxylic acids was investigated. The decarboxylation of 6-nitrobenzisoxazole-3-carboxylate anion would be a good probe to investigate the hydrophobic domains of polymer[5–7]. So using this reaction, the effects of alterations in pH, coordination to Cu(II) and composition of amino-organosiloxane/dimethyl siloxane copolymer are discussed in this report.

## EXPERIMENTAL

### *Materials*

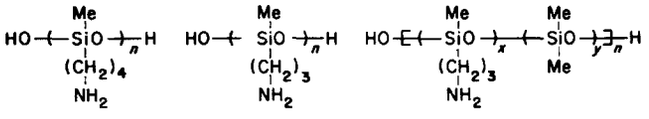

PABMS PAPMS I PAPMS II, III

The preparation of PAOS was described previously[8]. The characterizations are summarized in *Table 1*. All solutions were prepared with distilled and deionized water. $CuSO_4 \cdot 5H_2O$, ascorbic acid, *p*-hydroquinone and $NaClO_4$ were purchased from Kanto Chemicals and were used without further purification. 6-Nitrobenzisoxazole-3-carboxylic acid was prepared according to the method of Borche, and recrystallized from methanol, m.p. 167–169°C (literatuve value 167–169°C)[9].

### *Methods*

*Catalytic activity of oxidation.* All spectrophotometric determinations were made on a Shimazu UV-240 thermostated spectrophotometer. The solutions were saturated with pure oxygen by bubbling prior to addition of the substrate. In the kinetic experiments, initial rates were determined for each substrate concentration. All kinetics were followed at 25°C.

(*1*) *Ascorbic acid.* The rate of ascorbate oxidation was followed spectrophotometrically at 265 nm as described earlier[10]. The molar extinction coefficient of ascorbic acid at pH 4.3 was $\varepsilon = 13000$ mol$^{-1}$ cm$^{-1}$ (ref. 11).

(*2*) p-*Hydroquinone.* *p*-Hydroquinone oxidation to the quinone was followed spectrophotometrically at 240 nm.

0032–3861/86/020293–06$03.00

**Table 1** Characterization of poly(amino-organosiloxane)s (PAOS)

| Sample | DMS content[a] (mol%) | $\bar{M}_w$[b] | $\bar{M}_n$[b] | $M_w/M_n$ |
|---|---|---|---|---|
| PABMS | 0 | 31320 | 25740 | 1.22 |
| PAPMS I | 0 | 5750 | 4430 | 1.30 |
| PAPMS II | 40 | 14410 | 8150 | 1.77 |
| PAPMS III | 50 | 30400 | 12090 | 2.51 |

[a] Determined by $^1$H n.m.r. spectra
[b] Determined by g.p.c.

Hydroquinone ($H_2Q$) has a molar extinction coefficient of $\varepsilon = 475$ mol$^{-1}$ cm$^{-1}$ at this wavelength and the corresponding quinone has $\varepsilon = 2454$ mol$^{-1}$ cm$^{-1}$ at pH 4.3 (ref. 10). The change in *p*-$H_2Q$ concentration was calculated according to

$$\Delta[p\text{-}H_2Q] = \Delta A_{obs}^{240}/(\varepsilon_Q^{240} - \varepsilon_{H_2Q}^{240}) \quad (1)$$

where $\Delta A_{obs}^{240}$ is the change in absorbance at 240 nm and $\varepsilon_Q^{240}$ and $\varepsilon_{H_2Q}^{240}$ are the molar extinction of the quinone and hydroquinone respectively.

*Decarboxylation of 6-nitrobenzisoxazole-3-carboxylate anion* (**I**). Decarboxylation of (**I**) was studied by monitoring the difference between the absorption at 410 nm and that at 550 nm in a Shimazu UV-240 spectrophotometer. The reaction temperature was maintained at 25°C. Pseudo-first-order rate constants $k_0$ were calculated as in equation (2) by the method of least squares:

$$\ln\left(\frac{A_\infty - A_t}{A_\infty - A_0}\right) = k_0 t \quad (2)$$

where $A_t$, $A_0$ and $A_\infty$ refer to the differences in absorptions at time $t$, $t = 0$ and $t = \infty$ respectively. $A_\infty$ was calculated from $A_0$ and the absorption of a solution of 2-cyano-5-nitrophenol whose concentration was equal to that of the initial solution of (**I**).

## RESULTS AND DISCUSSION

*Ascorbic acid and hydroquinone oxidation*

The rate of oxidation of ascorbic acid and hydroquinone by PABMS–Cu(II) was followed as a function of the substrate concentration (*Figures 1, 2* and *3*).

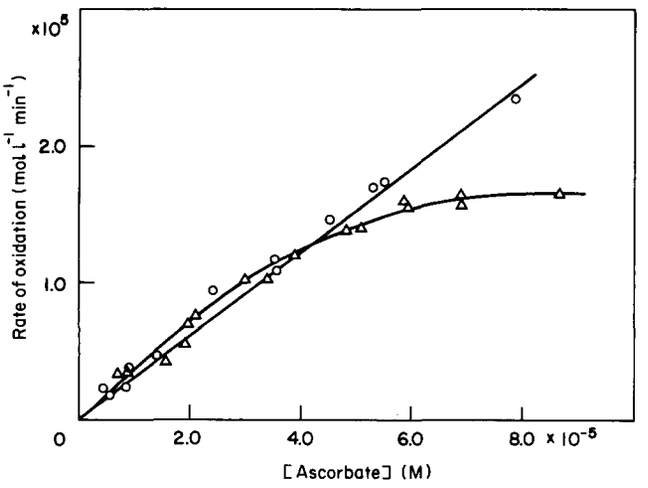


**Figure 1** Rate of oxidation as a function of substrate concentration: ascorbate oxidation in sodium acetate buffer; 0.02 M; pH 4.3; [Cu(II)], $6 \times 10^{-6}$ M; [PABMS], $4 \times 10^{-5}$ M (in amino residues). (–○–) Cu(II), (–△–) PABMS–Cu(II)

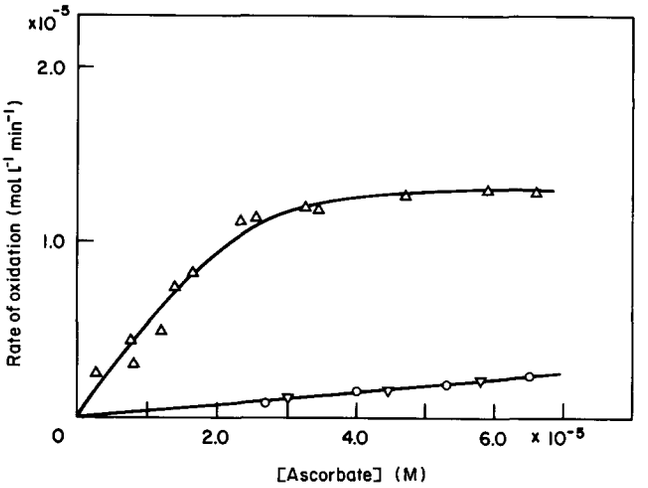


**Figure 2** Rate of oxidation as a function of substrate concentration: ascorbate oxidation in sodium acetate buffer; 0.02 M; pH 4.3; [Cu(II)], $6 \times 10^{-7}$ M; [PABMS], $4 \times 10^{-5}$ M (in amono residues). (–○–) Cu(II), (–△–) PABMS–Cu(II), (–▽–) PABMS–Cu(II) + 0.1 M $NaClO_4$

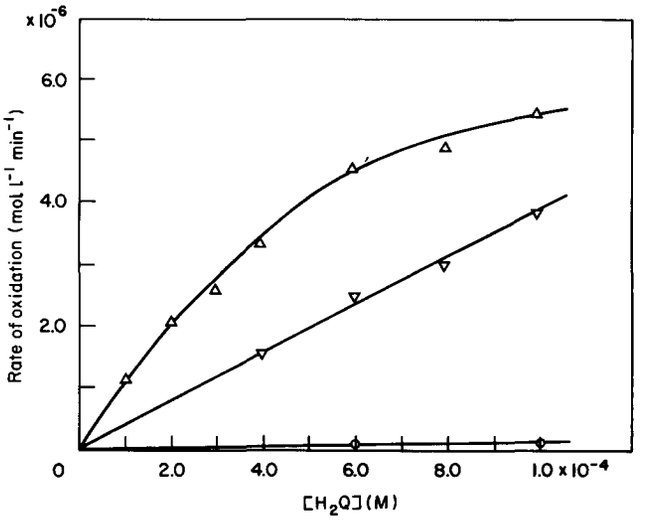


**Figure 3** Rate of oxidation as a function of substrate concentration: $H_2Q$ oxidation in sodium acetate buffer; 0.02 M; pH 4.3; [Cu(II)], $6 \times 10^{-6}$ M; [PABMS], $4 \times 10^{-5}$ M (in amino residues). (–○–) Cu(II), (–△–) PABMS–Cu(II), (–▽–) PABMS–Cu(II) + 0.1 M $NaClO_4$

The results were compared with the catalytic effect of the same concentrations of Cu(II) in the absence of PABMS. The rate of oxidation catalysed by PABMS–Cu(II) becomes independent of substrate concentration at relatively low concentration of the substrates. This typical Michaelis–Menten kinetic behaviour, which indicates the existence of a catalyst–substrate complex, is not exhibited by the aquoacetato complex in the same range of substrate concentrations. Assuming the existence of catalyst–substrate complex as an intermediate, the reaction mechanisms of PABMS–Cu(II) may be described by the following steps:

$$\text{PABMS–Cu(II)} + H_2A \underset{k_2}{\overset{k_1}{\rightleftharpoons}} \text{PABMS–Cu(II)–AH} + H^+ \quad (3)$$

$$\text{PABMS–Cu(II)–AH} \xrightarrow{k_3} \text{PABMS–Cu(I)} + \text{AH} \quad (4)$$

$$R = -\frac{d[H_2A]}{dt} = \frac{k_1 k_3 [\text{PABMS–Cu(II)}][H_2A]}{k_1[H_2A] + k_2[H^+] + k_3} \quad (5)$$

$$\frac{1}{R}=\frac{1}{k_3[\text{PABMS–Cu(II)}]}+\frac{k_2[H^+]+k_3}{k_1k_3[\text{PABMS–Cu(II)}][H_2A]} \quad (6)$$

where $H_2A$ represents the substrate and AH the radical produced on single equivalent oxidation. The plot of the reciprocal of the rate as a function of the reciprocal of the substrate concentration would give a straight line (*Figures 4* and *5*).

From the intercept of this line and its slope, one may derive $k_3$, the specific rate of decomposition of the substrate–catalyst complex, and the Michaelis constant $K_m=(k_2[H^+]+k_3)/k_1$ for this reaction. $K_m$, $V_{max}=k_3[\text{PABMS–Cu(II)}]$, and $k_3$ (known as the 'turnover number', i.e. the moles of substrate transformed per mole of catalyst per minute) are summarized in *Table 2*. The PABMS–Cu(II) catalysed reaction follows Michaelis–Menten kinetics because the terms $k_2[H^+]+k_3$ and $k_1[H_2A]$ are of the same order of magnitude. At pH 4.3, the amino groups of PABMS become cationic groups, and because of the electrostatic effect between positively charged PABMS and the negatively charged ascorbic acid ($pK=4.2$), $k_1[H_2A]$ becomes large[12,13]. $k_2$ may be somewhat small owing to the electrostatic repulsion of positively charged PABMS. Moreover, the concentration of $H^+$ ions in close vicinity of the positively charged PABMS is expected to be significantly lower in the bulk of the solution. Therefore the PABMS–Cu(II) catalysed reaction exhibits Michaelis–Menten kinetics. In the oxidation of neutral substrate *p*-$H_2Q$, $k_1[H_2A]$ is thought to become large, because of the hydrophobic interaction between *p*-$H_2Q$ and the hydrophobic domains of PABMS–Cu(II) complex. $k_2[H^+]$ may be small because of electrostatic repulsion, so Michaelis–Menten kinetics are observed. The value of $K_m$ for ascorbate ions is lower than that for hydroquinone (*Table 2*). If the $H_2A$ is negatively charged, its concentration in the vicinity of positively charged PABMS will be greater than within the bulk of the solution. This will lead to a further increase in the steady-state concentration of the PABMS–Cu(II)–AH complex. In order to clarify the electrostatic effect of PABMS, the effect of ionic strength on the rate of oxidation was investigated. The results are summarized in *Figures 2* and *3*. Sodium perchlorate was chosen since $ClO_4^-$ ions do not form stable complexes with monovalent or bivalent copper. Oxidations induced by the aquoacetato complexes of copper were found to be unaffected by inert salts. The addition of moderate concentration of inert salts changes the kinetic behaviour of the PABMS–Cu(II) catalysed reactions and the Michaelis–Menten behaviour disappears and the rate becomes equal to that of the Cu(II) catalysed reaction. From this phenomenon it can be assumed that the addition of inert electrolytes abolishes the electrostatic potential of PABMS. The effect of inert salts in the case of neutral *p*-$H_2Q$ oxidation is smaller than that for negatively charged ascorbate. These results indicate that substrates are incorporated by the electrostatic effect of PABMS and also by the hydrophobic interaction between the hydrophobic domains of PABS–Cu(II) complex. The effect of the concentration of Cu(II) ions on the PABMS–Cu(II) catalysed oxidation is presented in *Figures 1* and *2*. In *Figure 2*, the concentration of Cu(II) ion is one-tenth of that in *Figure 1*. In *Figure 1*, PABMS–Cu(II) catalysed reaction does not show high catalytic activity compared

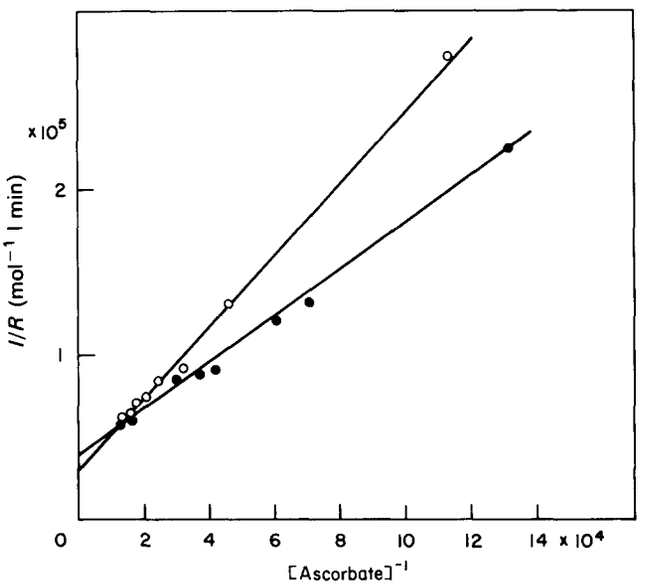


**Figure 4** Lineweaver–Burk plot of PABMS–Cu(II) catalysed oxidation. Experimental details as for *Figures 1* and *2* (–○–) Cu(II) $6\times10^{-6}$ M, (–●–) Cu(II) $6\times10^{-7}$ M

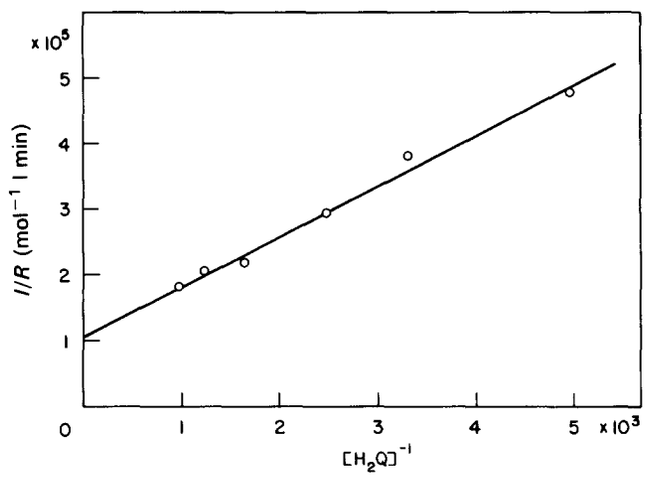


**Figure 5** Lineweaver–Burk plot of PABMS–Cu(II) catalysed oxidation. Experimental details as for *Figure 3*

**Table 2** Kinetic parameters for the PABMS–Cu(II) catalysed oxidation

| Catalyst | Substrate | $K_m$ (mol $l^{-1}$) | $V_{max}$ (mol $l^{-1}$ $min^{-1}$) | $k_3$[c] ($min^{-1}$) | r[d] |
|---|---|---|---|---|---|
| PABMS–Cu(II)[a] | Ascorbic acid | $7.7\times10^{-5}$ | $3.6\times10^{-5}$ | 6.0 | 1.2 |
| PABMS–Cu(II)[b] | Ascorbic acid | $3.7\times10^{-5}$ | $2.6\times10^{-5}$ | 43.0 | 13.8 |
| PABMS–Cu(II)[a] | *p*-Hydroquinone | $7.7\times10^{-4}$ | $1.0\times10^{-5}$ | 1.67 | 140 |

[a] [PABMS] $=4\times10^{-5}$ M. [Cu(II)] $=6\times10^{-6}$ M.
[b] [PABMS] $=4\times10^{-5}$ M. [Cu(II)] $=6\times10^{-7}$ M.
[c] $k_3$ (turnover number) = moles of substrate transformed per mole of copper per minute.
[d] $r=k_{obs}[\text{PABMS–Cu(II)}]/k_{obs}[\text{Cu(II)}]$; $k_{obs}$ is calculated graphically from the slope of the linear part of *Figures 1*, *2* and *3*.

with Cu(II) aquoacetate complex. On the other hand, in *Figure 2*, PABMS–Cu(II) catalysed reaction shows high catalytic activity, and the value of $k_{obs}$ is about 14-fold that of Cu(II) catalysed reaction and $k_3$ is very large (*Table 2*). In the case of high concentration of Cu(II), the conformation of PABMS becomes compact because of the crosslinked effect, which is attributed to coordination to Cu(II) ions. The active sites are covered with the hydrophobic domains of PABMS owing to this aggregation, and this compact form of PABMS prevents substrates from approaching active sites. Because of these effects, PABMS–Cu(II)–HA complexes cannot form easily. In the case of *Figure 2*, the effects of aggregation due to coordination are smaller than those in *Figure 1*. In this case, there are still so many positively charged amino residues that the electrostatic interactions between PABMS and substrates are stronger than those in *Figure 1*, so the PABMS–Cu(II)–HA complexes form easily. But around the active sites, the hydrophobic domains are formed by aggregation. The electron transfer reaction between substrates and Cu(II) ions may be enhanced, so $k_3$ is very large (equation (3)). In studies of the metal–polymer complex, some reports said that the hydrophobic interaction between polymer ligands and metals brought about the higher reactivities of electron transfer[14]. But in these studies, the hydrophobic domains formed by hydrophobic side chains have been discussed. On the other hand, in the case of PABMS–Cu(II) complex, the hydrophobic domains formed by main chains enhance the electron transfer reaction. Because of the flexibility of the PABMS main chain compared with carbon polymers, the aggregation due to coordination to Cu(II) is thought to be very sensitive. In the case of *Figure 2*, the electrostatic interaction between positively charged amino groups and substrates is strong, so the steady-state PABMS–Cu(II)–HA complexes form easily. What is more, the hydrophobic domains of PABMS–Cu(II) complex enhance the electron transfer reaction between substrates and Cu(II) ions. So the PABMS–Cu(II) catalysed oxidation shows high catalytic activity.

The viscosity behaviour of PABMS is shown in *Figure 6*. The reduced viscosity $\eta_{sp}/c$ of PABMS increases very rapidly with dilution. This viscosity behaviour of PABMS is similar to that of polyelectrolytes[15]. Owing to the electrostatic repulsion with the increase of the positive charge, the conformation of PABMS is thought to become loose. In the case of PABMS–Cu(II) complex, it will be noted that the sharp rise near zero is eliminated and the curve exhibits a maximum. With increasing added Cu(II) ion concentration, the values of $\eta_{sp}/c$ decrease, and the maximum shifts to a higher value of polymer concentration $C$. These results are explained by the crosslinked effect, which is attributed to coordination to Cu(II) ions. By this coordination, the loose PABMS conformation is inhibited, and the conformation of PABMS becomes compact. It is also found that this aggregation effect is enlarged with an increase in Cu(II) concentration.

*PAOS catalysed decarboxylation*

The ability to coordinate to metal, the electrostatic effect of positively charged amino groups and the hydrophobicity and flexibility of the main chain of PAOS are thought to enhance the catalytic efficiency towards oxidation. The effects of these three factors on the

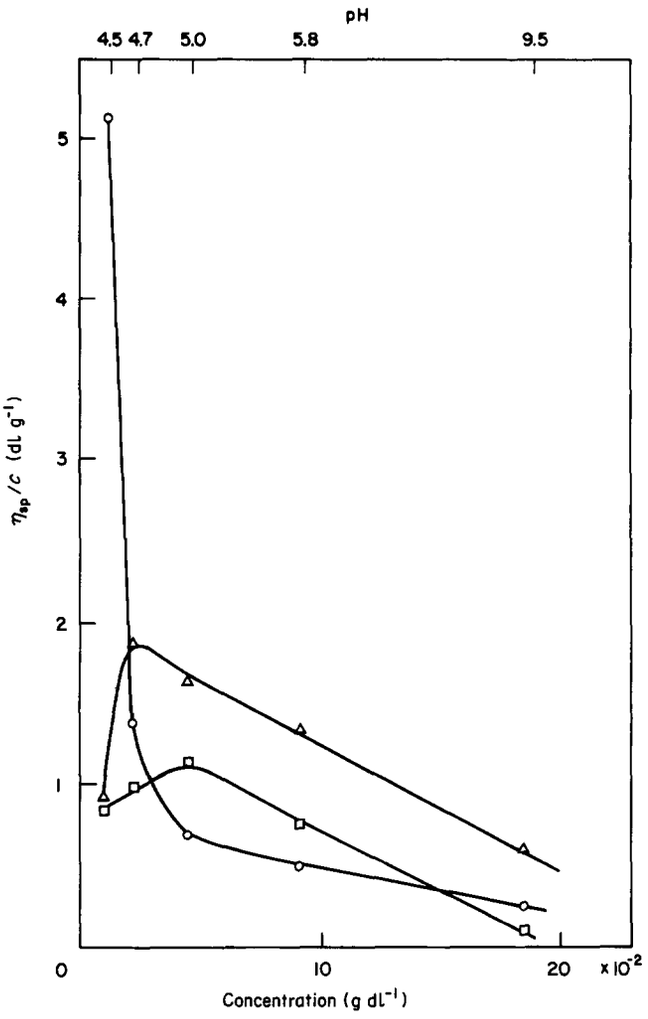


**Figure 6** Viscosity behaviour of PABMS and PABMS–Cu(II) complex in aqueous solution. The solution was diluted with 0.02 M sodium acetate buffer (pH 4.3). (-○-) PABMS, (-△-) PABMS + Cu(II) [100:1], (-□-) PABMS + Cu(II) [100:2]

conformation of PAOS in aqueous solution were studied by using decarboxylation. The decarboxylation of 6-nitrobenzisoxazole-3-carboxylate anion (I) is unimolecular, free from acid and base catalysers[5-7]. This

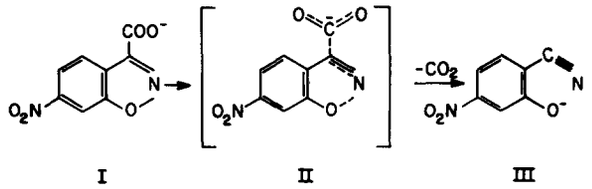


I II III

decarboxylation is a good probe to investigate the hydrophobic environments around active sites. The hydrophobic environment stabilizes the charge delocalized transition state of the benzisoxazole carboxylate anion and thereby accelerates the rate of decarboxylation. The observed rate constant $k$ of decarboxylation of (I) was followed as a function of PAPMS I concentration (*Figure 7*). The value of $k$ rises rapidly and finally a plateau is obtained. This saturation behaviour of the rate constant is similar to that reported by Kunitake[4]. At pH 4.3, owing to the protonation at amino groups, the amino groups of PABMS I become cationic sites. On the other hand, the main chain of PAPMS I is hydrophobic. So PAPMS I seems to be like

polysoap. The hydrophobic domains formed by PAPMS I main chains enhance the decarboxylation of (I). The rate constants of PAPMS I–Cu(II) complex are larger than those of PAPMS I at each polymer concentration. This result indicates that large amounts of hydrophobic domains are formed by coordination to Cu(II) ions. The rate constants of decarboxylation of (I) at pH 4.3 are summarized in *Table 3*. At pH 4.3, the amino groups of PAOS become positively charged and the conformation of PAOS is thought to be loose owing to electrostatic repulsion between positively charged groups. It is not easy for the homopolymer of PAOS (PAPMS I) to form hydrophobic domains because of electrostatic repulsion between neighbouring cationic sites. On the other hand, in the case of amino-organosiloxane/dimethyl siloxane (AOS/DMS) copolymer (PAPMS II, III), the repulsion is weakened and the hydrophobic domains are formed more easily by introducing DMS. The rate constant rises with increase of the DMS content, so the introduction of DMS into PAOS greatly affects the formation of hydrophobic domains. The loose conformation of PAOS is inhibited by coordination to Cu(II) ions and becomes compact. This is the reason why, in the case of PAOS–Cu(II) complex, the rate constants are larger than those of PAOS with each polymer. The flexibility of the PAOS main chain contributes to this sensitive aggregation effect. The rate constants for decarboxylation of (I) at pH 7.0 are summarized in *Table 4*. In this case, the concentration of polymer is half that at pH 4.3, nevertheless the rate constants are larger than at pH 4.3 with each PAOS. This indicates that the hydrophobic domains increase with a rise in pH value. In pH 7.0, a small number of the amino groups of PAOS become positively charged groups[16,17], and electrostatic repulsion is weakened. Owing to either the hydrophobic interaction between main chains of PAOS or the flexibility of the PAOS main chain, the conformation of PAOS becomes compact, so the hydrophobic domains are formed to a great extent. Similar to pH 4.3, the rate constants increase with increase of the DMS content. At pH 7.0, the hydrophobic domains are also formed by coordination to Cu(II), but this aggregation effect is not remarkable in comparison with pH 4.3. This result can be explained by the decrease of electrostatic repulsion, which enables the conformation of PAOS to be compact owing to the hydrophobic interaction between the main chains. Since the conformation of PAOS has already become compact, the aggregation effect is not remarkable as for pH 4.3.

The hypsochromic shift of absorption maximum of methyl orange was studied to investigate the hydrophobic domains of PAOS in aqueous solution. Methyl orange has $\lambda_{max}$ at 465 nm, whereas an apolar environment causes a shift of $\lambda_{max}$ to shorter wavelengths. The results are summarized in *Table 5*. At pH 5.0, the hypsochromic shift was not observed for PAPMS I, III or PAPMS–Cu(II) complex, but PAPMS III–Cu(II) complex caused a shift of $\lambda_{max}$. At pH 7.0, the hypsochromic shift was observed for all PAOS and PAOS–Cu(II) complexes. These results also indicate that alterations in pH and coordination to Cu(II) affect the conformation of PAOS.

In conclusion, owing to the flexibility and hydrophobicity of the PAOS main chain, the conformation of PAOS in aqueous solution is controlled easily by coordination to metal ions and by electrostatic effects. Hydrophobic interactions between PAOS main chains can also control the conformation of PAOS, and PAOS form the hydrophobic domains. Owing to these factors, the PAOS–Cu(II) complex exhibits high catalytic activity in certain oxidation and decarboxylation reactions. Although the mechanisms of reaction of enzyme and PAOS–Cu(II) complexes are evidently different, the specific effect of these factors demonstrated in this study may perhaps contribute to certain enzymic reactions.

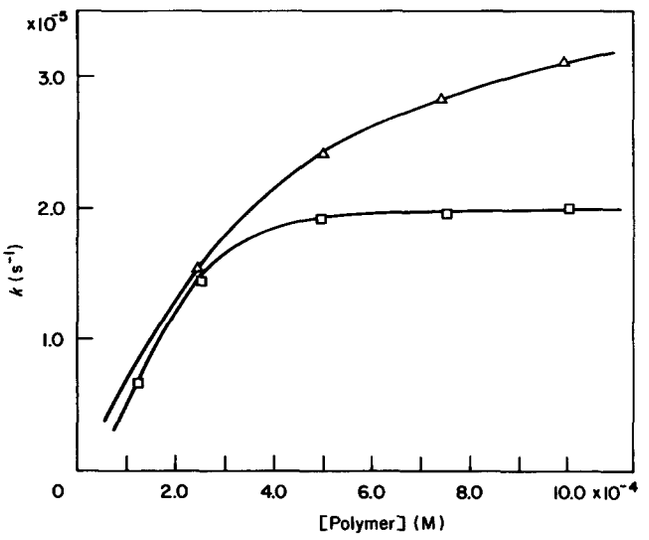


**Figure 7** Decarboxylation rate constant plotted against the concentration of PAPMS I polymer: [substrate], $1.0 \times 10^{-4}$ M; pH 4.3; 0.02 M sodium acetate buffer. (–□–) PAPMS I, (–△–) PAPMS I–Cu(II) and PAPMS I/Cu(II) = 10/1

**Table 3** Decarboxylation rate constants at pH 4.3

| Sample | $k \times 10^4$ ($s^{-1}$) | Sample | $k \times 10^4$ ($s^{-1}$) |
|---|---|---|---|
| PAPMS I | 0.20 | PAPMS I–Cu(II) | 0.31 |
| PAPMS II | 0.57 | PAPMS II–Cu(II) | 0.79 |
| PAPMS III | 1.15 | PAPMS III–Cu(II) | 1.81 |

25°C, pH 4.3 with 0.02 M sodium acetate buffer, [polymer] = $1.0 \times 10^{-3}$ M, [substrate] = $1.0 \times 10^{-4}$ M, [Cu(II)] = $5.0 \times 10^{-5}$ M; without polymer, $k_0 = 5.28 \times 10^{-6}$ ($s^{-1}$)

**Table 4** Decarboxylation rate constants at pH 7.0

| Sample | $k \times 10^4$ ($s^{-1}$) | Sample | $k \times 10^4$ ($s^{-1}$) |
|---|---|---|---|
| PAPMS I | 0.83 | PAPMS I–Cu(II) | 1.11 |
| PAPMS II | 1.16 | PAPMS II–Cu(II) | 1.60 |
| PAPMS III | 1.95 | PAPMS III–Cu(II) | 2.09 |

25°C, pH 7.0 with 0.01 M Tris–HCl buffer, [polymer] = $5.0 \times 10^{-4}$ M, [substrate] = $1.0 \times 10^{-4}$ M, [Cu(II)] = $5.0 \times 10^{-5}$ M; without polymer, $k_0 = 4.67 \times 10^{-6}$ ($s^{-1}$)

**Table 5** Hypsochromic shift of absorption maximum of methyl orange

| Catalyst | Shift at pH 5.0 (nm) | Shift at pH 7.0 (nm) |
|---|---|---|
| PAPMS I | 465 | 463 |
| PAPMS I–Cu(II) | 465 | 463 |
| PAPMS III | 465 | 457 |
| PAPMS III–Cu(II) | 457 | 457 |
| without polymer | 465 | 465 |

[Polymer] = $1.43 \times 10^{-3}$ M, [methyl orange] = $1.30 \times 10^{-3}$ M, [Cu(II)] = $2.1 \times 10^{-4}$ M

## ACKNOWLEDGEMENT

The authors thank the Chisso Corporation, which supplied the organosiloxanes used in this work.

## REFERENCES

1 Andrianov, K. A. and Slonimski, G. L. *J. Polym. Sci.* 1972, **10**, 1–22
2 Niino, M., Veno, Y., Arabi, T. and Sekine, Y. *Polymer* 1983, **24** (*Commun.*), 124
3 Bachrach, A. and Zilkha, A. *Eur. Polym. J.* 1984, **20**, 493
4 Kunitake, T. and Shinkai, S. *J. Org. Chem.* 1977, **42**, 306
5 Bunton, C. A. and Minch, M. J. *J. Am. Chem. Soc.* 1973, **95**, 3263
6 Yamazaki, N. and Nakahama, S. *Polym. J.* 1980, **12**, 231
7 Bunton, C. A. *Tetrahedron Lett.* 1976, 3881
8 Koyama, N., Sekiyama, Y., Veno, Y. and Sekine, Y. *Polymer* 1985, **26** (*Commun.*), 139
9 Borche, W. *Ber. Bunges*, 1909, **42**, 1310
10 Racker, E. *Biochem. Biophys. Acta* 1952, **9**, 577
11 Pecht, I. and Levitski, A. *J. Am. Chem. Soc.* 1967, **89**, 1587
12 Meider, H. C. and Park, N. *Makromol. Chem.* 1977, **179**, 1019
13 Skurlatov, Y. I. and Konver, V. Y. *Eur. Polym. J.* 1979, **15**, 811
14 Tsuchida, E. and Shigehara, K. *J. Polym. Sci., Polym. Chem. Edn.* 1979, **13**, 1457
15 Fuoss, R. M. and Strauss, O. P. *J. Polym. Sci.* 1948, **3**, 602
16 Kimura, K. and Inaki, Y. *Makromol. Chem.* 1974, **175**, 83
17 Inaki, Y. and Kimura, K. *Makromol. Chem.* 1973, **171**, 19